

# The structure of convective rain cells at mid-latitudes

N. Rebora<sup>1</sup> and L. Ferraris<sup>1,2</sup>

<sup>1</sup>CIMA, University of Genoa and University of Basilicata, Savona, Italy

<sup>2</sup>DIST, University of Genoa, Genoa, Italy

Received: 11 November 2005 – Revised: 23 November 2005 – Accepted: 6 December 2005 – Published: 23 January 2006

**Abstract.** Rain cells are structures which represent an important component of convective precipitation and a study of their properties represents a necessary step both towards improved stochastic models of small-scale precipitation and for the verification of deterministic high resolution local-area models. The case of intense convective precipitation in the tropics has been analysed in a recent study (von Hardenberg et al., 2003). Here we extend the analysis to mid-latitudes and we present results on the structure of convective rain cells observed by radar measurements in Italy. In particular we consider the average shape of precipitation cells and its dependence on radar resolution and the distributions of ellipticities.

## 1 Introduction

Intense rainfall events, both in the tropics and at midlatitudes, are dominated by the presence of convective rain cells. These structures may cause sudden floods in small catchments typical of the Mediterranean environment and various hydrogeological natural disasters in these areas and in the Alps have been linked to strong convective precipitation (Hagen et al., 2000).

The study of the spatio-temporal structure of rain cells can be of relevance for the development of stochastic techniques for precipitation nowcasting or downscaling (Ferraris et al., 2003) and for improving and verifying deterministic high-resolution limited area models (Parodi, 2005).

Rain cells are intense rainfall structures with spatial dimensions of about 5–10 km that appear to be embedded in regions of more widespread rainfall. The cells tend to last around 30 min and to produce a peak precipitation of about 50–100 mm/h (Austin and Houze, 1972).

One of the basic properties of rain cells is the distribution of the precipitation around the intensity peak. This dis-

tribution, i.e. the "shape" of the rain cell, is an important free parameter for stochastic models for nowcasting or downscaling (e.g. LeCam, 1961; Waymire et al., 1984; Eagleson et al., 1987; Anagnostou and Krajewski, 1997). Different shapes have been proposed in the past: simple top-hat profiles (Cox and Isham, 1988; Wheeler et al., 2000), Gaussian (Waymire et al., 1984; Eagleson et al., 1987), power-law (Ferraris et al., 2003) or exponential shapes (Capsoni et al., 1987). Non-gaussian cell shapes have been used in some stochastic rainfall models proposed both for hydrological purposes and for studies on propagation of electromagnetic waves; However only few works delved into the issue of determining the shape of these cells directly from observed radar rainfall fields (Feral et al., 2000; von Hardenberg et al., 2003).

In this work, we extend to mid-latitude radar observations the analysis procedure used by von Hardenberg et al. (2003) for tropical convective precipitation data, by considering a set of precipitation fields measured by an Italian meteorological radar. We identify the cells' centers and we analyze the spatial distribution of precipitation intensity around each center. We show the effect of changing radar resolution and rainfall estimation algorithm on some cells properties such as ellipticities, precipitation volumes, peak intensities and shape found for the precipitation cores. The results are compared with the previous results obtained from the tropical TOGA-COARE dataset analysis.

## 2 Radar datasets

We consider precipitation fields measured by the C-band, polarimetric (C-POL) radar of Mount Settepani located between the Liguria and Piemonte regions in North-Western Italy. The event considered here was measured on 23 November, 2003, starting from 00:00 UTC. The event has a total duration of about 48 h and an average rainfall intensity of 2.5 mm/h with peaks larger than 150 mm/h. We selected this specific event because it is a typical example of intense

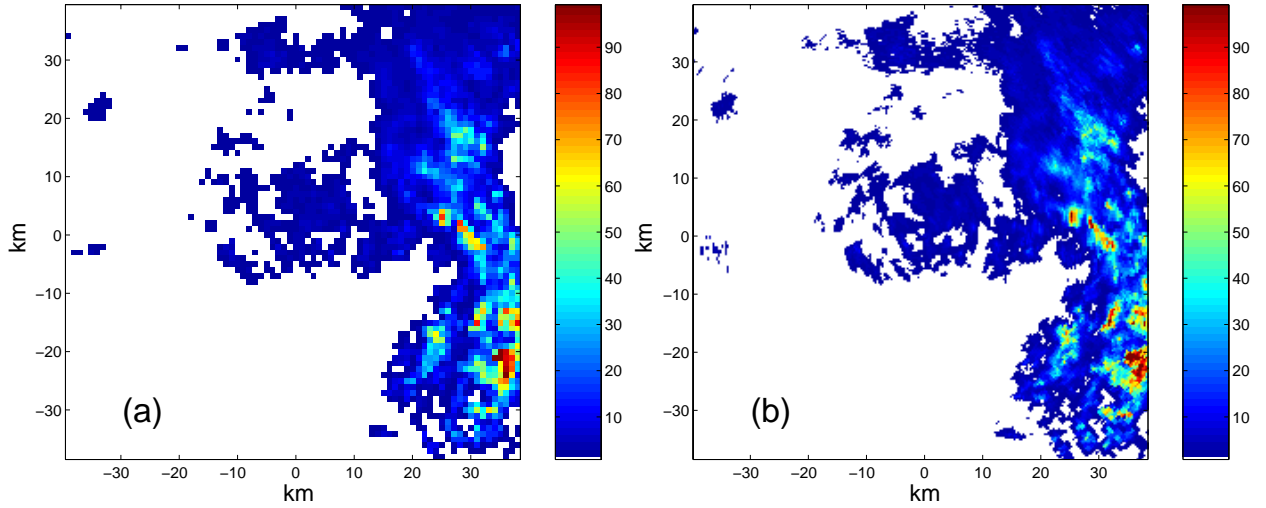


**Fig. 1.** Example of precipitation fields measured by Mount Settepani radar. Panel (a) shows a  $1\text{ km} \times 1\text{ km}$  field (low-resolution) while in panel (b) the corresponding high-resolution ( $300\text{ m} \times 300\text{ m}$ ) precipitation map, is presented. The colorbars indicate the precipitation intensity in mm/h.

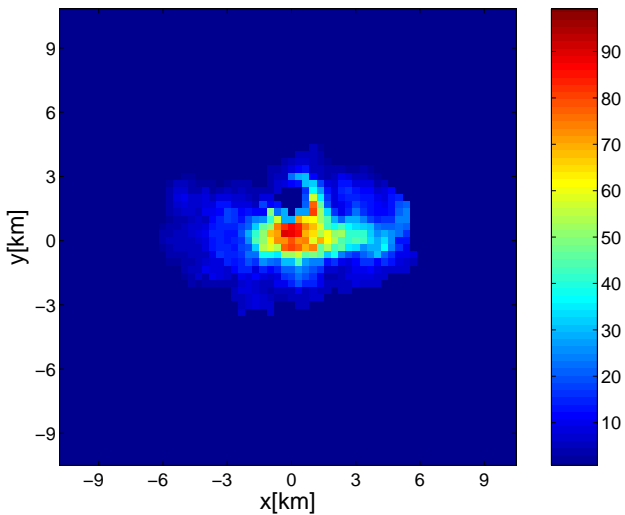


**Fig. 2.** Example of high-intensity precipitation cell measured by Mt. Settepani radar. The colorbar indicates the precipitation intensity in mm/h.

fall precipitation at mid-latitudes and it includes a strong convective component.

The radar data considered here are measured every 10 min at two different spatial resolutions, 300 m and 1 km. We create three precipitation datasets by using both high- and low-resolution reflectivity ( $Z$ ) and differential reflectivity ( $Z_{dr}$ ) fields:

- $Z$ - $R$  dataset, called LR1. The precipitation field, at a resolution of 1 km in space and 10 min in time, has been derived from  $Z$  measurements by using the Marshall-Palmer relationship ( $R(Z)=0.0365Z^{0.625}$ ).

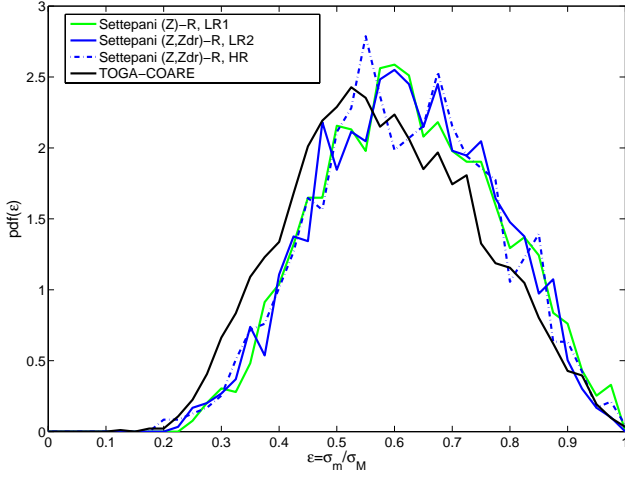
- $(Z, Z_{dr})$ - $R$  dataset (low resolution), called LR2. The precipitation field, at a resolution of 1 km in space and 10 min in time, has been derived by applying the following blended algorithm that accounts for both  $Z$  and  $Z_{dr}$ :  $R(Z, Z_{dr})=0.0058Z^{0.91}10^{0.209Z_{dr}}$  (Bringi and Chandrasekar, 2001).
- $(Z, Z_{dr})$ - $R$  dataset (high resolution), called HR. The precipitation field, at a resolution of 300 m in space and 10 min in time, has been derived by using the blended algorithm described above.

Figure 1 shows an example of high- and low-resolution precipitation fields obtained by using the  $(Z, Z_{dr})$ - $R$  algorithm.

As a reference data set we consider also spatial maps of precipitation intensity measured during the TOGA-COARE campaign (Short et al., 1997). These fields have been obtained from radar reflectivity maps at a spatial-temporal resolution of 2 km and 10 min in the period from November 1992 to February 1993.

### 3 The shape of mid-latitude convective cells

Rain cells are identified separately in each spatial frame of the precipitation fields, by applying the procedure described in von Hardenberg et al. (2003) to the four datasets presented in the previous section. In short, this procedure follows two steps: (1) identification of local intensity maxima with values larger than 10 mm/h; (2) identification of all contiguous pixels that belong to a given maximum. The procedure stops when minimum threshold of 5 mm/h is reached. For further details and a complete description of the algorithm we refer to von Hardenberg et al. (2003).



**Fig. 3.** Distribution of rain cells ellipticities. The different lines refer to the four datasets considered: *light, green line*, Z-R, low-resolution (LR1) dataset; *continuous blue line*: (Z, Z<sub>dr</sub>)-R, low resolution (LR2) dataset; *dashed blue line*: (Z, Z<sub>dr</sub>)-R, high-resolution dataset (HR); *black line*: TOGA-COARE.

The procedure identifies 1557 rain cells for the LR1 dataset, 1192 rain cells for the LR2 dataset, 947 rain cells for HR dataset and 3740 rain cells for TOGA-COARE fields. As an example, Fig. 2 shows a precipitation cell extracted from the high-resolution precipitation fields (HR dataset).

The selected rain cells are characterized by different orientations, areas, ellipticities and total precipitation volumes. We use the lengths of the two principal moments of inertia of each cell,  $\sigma_M$  and  $\sigma_m$ , to characterize the lengths of the major and minor axes respectively.

The distributions of ellipticities,  $\epsilon = \sigma_m / \sigma_M$  of the cells are reported in Fig. 3. As is clear from this figure, both the choice of the algorithm used for precipitation estimation and spatial resolution have not a significant effect on the cells axis ratio. TOGA-COARE cells have a distribution which is only slightly shifted towards lower ellipticities with respect to the distributions for Mt. Settepani fields. The average ellipticity of the TOGA-COARE rain cells is  $\bar{\epsilon} = 0.59$  and the median value is  $\epsilon_0 = 0.57$ ; for the LR2 dataset we have  $\bar{\epsilon} = 0.62$  and  $\epsilon_0 = 0.62$ , similar results are obtained for the other dataset considered. To complete the overview on the properties of precipitation cells, in Fig. 4 are shown the probability distributions of precipitation volumes (upper panel) and the distributions of peak intensities (lower panel).

In order to obtain an average shape characterizing cells in each field, we follow the same procedure as in von Hardenberg et al. (2003). Each rain cell is rotated aligning its major and minor axes with the same directions. The  $i$ -th cell in the rotated reference system can be written as

$$R_i(x, y) = V_i \Phi_i(r, \theta), \quad (1)$$

where  $V_i$  is the cell rainfall volume and  $\Phi_i(r, \theta)$  is a function that represents the shape of the cell as a function of the radial

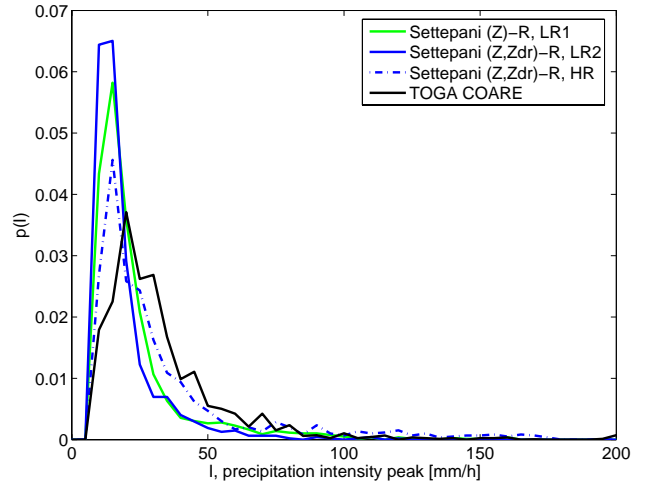
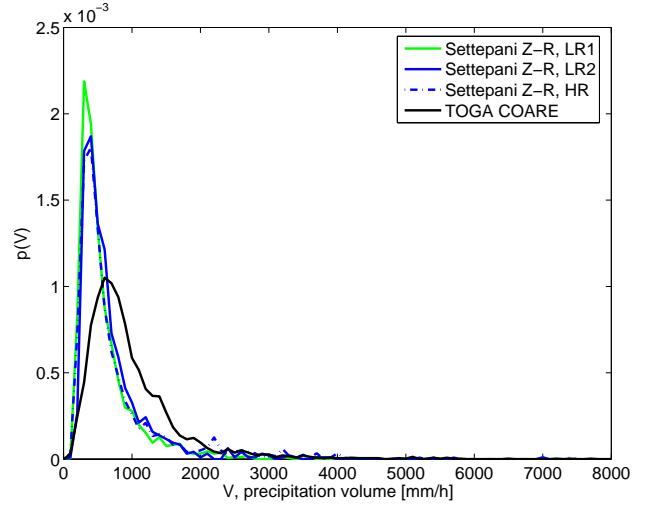


**Fig. 4.** Distribution of rain cells precipitation volumes (upper panel) and distribution of rain cells intensity peaks (lower panel). The different lines refer to the four datasets considered: *light, green line*, Z-R, low-resolution (LR1) dataset; *continuous blue line*: (Z, Z<sub>dr</sub>)-R, low resolution (LR2) dataset; *dashed blue line*: (Z, Z<sub>dr</sub>)-R, high-resolution dataset (HR); *black line*: TOGA-COARE.

distance from the cell center,  $r = \sqrt{x^2 / \sigma_M^2 + y^2 / \sigma_m^2}$ , and of the angular coordinate,  $\theta$  in the rotated reference frame. Accordingly the average cell shape can be obtained by rescaling the rotated cells to have unitary volume and rescaling the major and minor axes to unitary lengths. These rescaled and normalized cells can then be averaged to find an average shape  $\Phi(r, \theta)$ . Figure 5 reports the function  $\Phi(r, \theta)$  for the cells extracted from the LR2 dataset that indicates a non-Gaussian distribution of precipitation intensity around the cell center. The radial average  $\phi(r)$  of the rain cell shape  $\Phi(r, \theta)$  is reported in Fig. 6 for all the four datasets considered in this work. The inset shows the same results in log-normal coordinates where a perfect exponential shape would be represented by a straight line. The averaged cell profiles are exponential over more than one order of magnitude in amplitude. Some differences between the four profiles are however

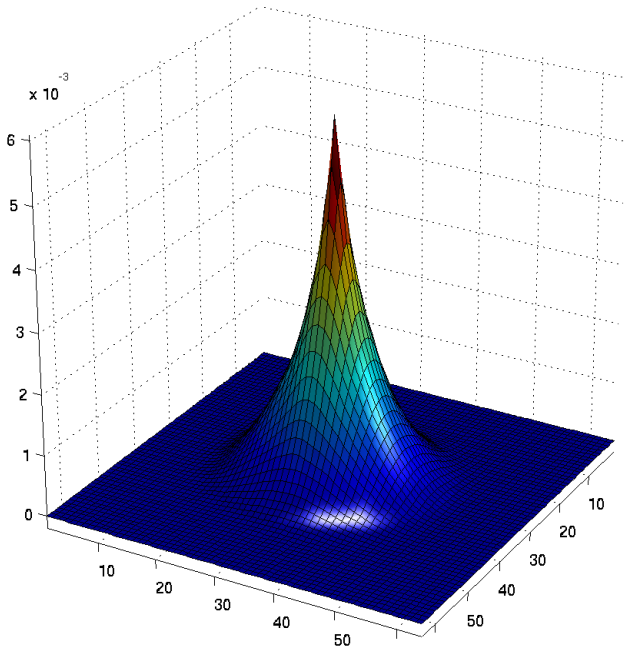


**Fig. 5.** Average shape of cells extracted from the LR2 dataset.

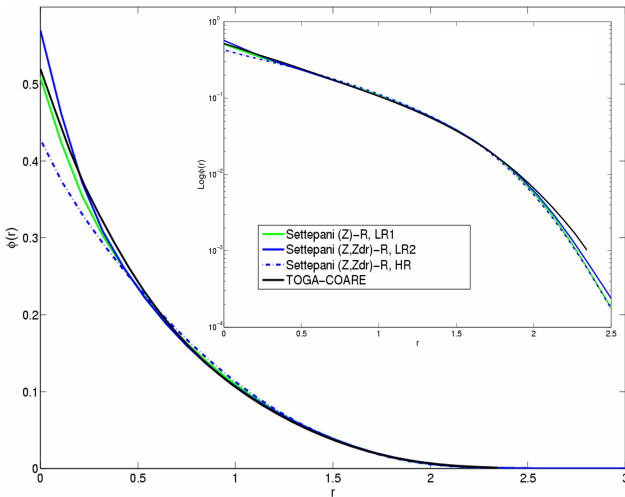


**Fig. 6.** The radial-averaged rainfall intensity profiles for the four datasets considered in this work. The different lines refer to the four datasets considered: *light, green line*,  $Z$ - $R$ , low-resolution (LR1) dataset; *continuous blue line*:  $(Z, Z_{dr})$ - $R$ , low resolution (LR2) dataset; *dashed blue line*:  $(Z, Z_{dr})$ - $R$ , high-resolution dataset (HR); *black line*: TOGA-COARE.

present; future works will be devoted on investigating the dependence of rain cells shape on spatial resolution and on algorithms for precipitation estimation.

#### 4 Conclusions

This preliminary work aims at investigating the behavior of mid-latitudes precipitation cells measured by a meteorological radar.

To evaluate the sensitivity of cell properties (ellipticity, volume, intensity peak and shape) to different methods of rainrate estimate and to radar resolution, we compare cells extracted from three different datasets derived from the same event measured by Mt. Settepani radar in North-Western Italy where two different rainrate estimate methods and two different resolutions were used. As reference dataset we use the rainfall fields measured during the TOGA-COARE campaign.

From this preliminary analysis we may conclude that the distributions of ellipticities, precipitation volumes and intensity peaks are not significantly sensitive to changes in radar resolution and do not have a clear dependence on the algorithm chosen for estimating rainrate field. The ellipticity distributions found for Mt. Settepani rain cells are also very close to that obtained for the tropical precipitation cells measured during the TOGA-COARE campaign.

The mid-latitude precipitation cells considered in this work show an average cell shape that is close to an exponential profile. This result is consistent with those derived from the analysis of tropical precipitation cells (von Hardenberg et al., 2003). Future work will be devoted on investigating the dependence of rain cells shape on spatial resolution and on algorithms for precipitation estimation that use a full set of polarimetric variables.

*Acknowledgements.* We thank F. Marzano, J. von Hardenberg, M. Montopoli and F. Silvestro for interesting discussions. This work has been supported by Regione Liguria. We acknowledge also Regione Liguria and Regione Piemonte for providing us with data of Mt. Settepani polarimetric radar.

Edited by: V. Kotroni and K. Lagouvardos

Reviewed by: S. Michaelides

#### References

- Anagnostou, E. and Krajewski, W. F.: Simulation of radar reflectivity fields: Algorithm formulation and evaluation, *Water Resour. Res.*, 33, 1419–1428, 1997.
- Austin, P. and Houze, R.: Analysis of structure of precipitation patterns in New England, *J. Appl. Meteorol.*, 11, 926–934, 1972.
- Bringi, V. and Chandrasekar, V.: *polarimetric doppler weather radar, principles and applications*, Cambridge university Press, Cambridge, 2001.
- Capsoni, C., Fedi, F., Magistroni, C., Paraboni, A., and Pawlina, A.: Data and theory for a new model for the horizontal structure of rain cells for propagation applications, *Radio Sci.*, 22, 395–404, 1987.
- Cox, D. R. and Isham, V.: A simple spatio-temporal model of rainfall, *Proc. R. Soc. Lond.*, 415(A), 317–328, 1988.
- Eagleson, P., Fennessey, N., Quiliang, W., and Rodriguez-Iturbe, I.: Application of spatial Poisson models to airmass thunderstorm rainfall, *J. Geophys. Res.*, 92(D8), 9961–9978, 1987.
- Feral, L., Mesnard, F., Sauvageot, H., Castanet, L., and Lemorton, J.: Rain Cells Shape and Orientation Distribution in South-West France, *Phys. Chem. Earth B*, 25, 1073–1078, 2000.

- Ferraris, L., Gabellani, S., Rebora, N., and Provenzale, A.: A comparison of stochastic models for spatial rainfall downscaling, *Water Resour. Res.*, 39, 1368–1384, 2003.
- Hagen, M., Schiesser, H.-H., and Dorninger, M.: Monitoring of mesoscale precipitation systems in the Alps and the northern alpine foreland by radar and rain gauges, *Meteorol. Atmos. Phys.*, 72, 87–100, 2000.
- LeCam, L.: A stochastic description of precipitation, in *Proc. 4th Berkeley symposium on mathematical statistics and probability*, Vol 3, pp. 125–151, University of California Press, 1961.
- Parodi, A.: Dynamics of intense convective rain cells, *Adv. Geosci.*, 2, 1–6, 2005.
- Short, D. A., Kucera, P. A., Ferrier, B. S., Gerlach, J. C., Rutledge, S. A., and Thiele, O. W.: Shipboard Radar Rainfall Patterns within the TOGA COARE IFA, *Bull. Am. Met. Soc.*, 78, 2817–2836, 1997.
- von Hardenberg, J., Ferraris, L., and Provenzale, A.: The shape of convective rain cells, *Geophys. Res. Lett.*, 30, 10.1029/2003GL018539, 2003.
- Waymire, E., Gupta, V., and Rodriguez-Iturbe, I.: A spectral theory of rainfall intensity at the meso-beta scale, *Water Resour. Res.*, 20, 1483–1465, 1984.
- Wheater, H., Isham, V., Cox, D., Chandler, R., Kakou, A., Northrop, P., Oh, L., Onof, C., and Rodriguez-Iturbe, I.: Spatial-temporal rainfall fields: modelling and statistical aspects, *Hydrol. Earth Syst. Sci.*, 4, 581–601, 2000.